10. P. A. Reasenberg, *J. Geophys. Res.* **90**, 5479 (1985).
11. Data were obtained from catalogs prepared separately for southern and eastern California (*12*), northern California before 1971 (*13*), and northern California after 1971 (*14*). A variety of magnitude scales have been used in California. For mainshocks ($M \geq 5.0$), $M_W$ (moment magnitude) was used when available; otherwise $M_L$ (local magnitude) was used. For southern and eastern California aftershocks, we used $M_L$ for ($M \geq 3.0$), and $M_{CA}$ (coda amplitude magnitude) for ($M < 3.0$). For northern California aftershocks, we used $M_L$ before 1970 and $M_D$ (coda duration amplitude) after 1970.
12. D. D. Given, L. K. Hutton, L. M. Jones, *U.S. Geol. Surv. Open-File Rep. 87-488* (1987).
13. R. B. Darragh *et al.*, *Bull. Seismographic Stations Univ. Calif., Berkeley* **55**, 1–2 (1985).
14. S. L. Kirkman-Reynolds and F. W. Lester, *U.S. Geol. Surv. Open-File Rep. 86-157* (1987).
15. This algorithm identifies clusters of earthquakes in time and space. By defining the identified clusters as the set of aftershocks, we effectively eliminate the spatial part of the problem. Thus, from this point on, the analysis considers aftershocks as two-dimensional (time-magnitude) vectors.
16. We used $c = 0.05$ days, the value that minimizes $\chi^2$ for the post-1970 data.
17. Errors are ±1 standard deviation of the mean.
18. Subsets of sequences occurring in each tectonic regime in California were compared with the two-sample *t* test for difference in the mean of each parameter; $\bar{a}_{\text{east}} > \bar{a}_{\text{north}}$, $p < 0.02$ and $\bar{a}_{\text{east}} > \bar{a}_{\text{south}}$, $p < 0.005$.
19. Sensitivity of the calculated probabilities to variations in the model parameters was investigated. A 10% increase in *a*, *b*, *c*, or *p*, relative to the generic value, leads to probabilities for strong aftershocks at $S = 1$, $(T - S) = 365$ of 0.44, 0.35, 0.32, and 0.25, respectively, compared to the generic probability of 0.32 in Table 1. Corresponding probabilities for larger mainshocks are 0.068, 0.042, 0.046 and 0.035, compared to the generic probability 0.046 in Table 1.
20. L. M. Jones and P. A. Reasenberg, *Eos* **69**, 1305 (1988).
21. J. Bennett and R. Sherburne, Eds., *Calif. Div. Mines Geol. Spec. Pub. 66* (1983).
22. E. Hauksson *et al.*, *Science* **239**, 1409 (1988).
23. W. Ellsworth and M. Rymer, Eds., *U.S. Geol. Surv. Prof. Pap. 1487* (1988).
24. We obtained the probability estimates given in Table 2 using parameters estimated for the entire earthquake sequences; thus, they are generally better-determined than those that would have been obtained in real-time during the earthquake sequences. We present these best model estimates of aftershock probability rather than the real-time or "limited knowledge" estimates in order to best demonstrate the time- and magnitude-dependence of the calculated probabilities and to provide a uniform comparison of results for these contrasting earthquake sequences.
25. R. T. Hogg and A. T. Craig, *Introduction to Mathematical Statistics* (Macmillan, New York, 1978).
26. A. H. Bowker and G. J. Lieberman, *Engineering Statistics* (Prentice Hall, Englewood Cliffs, New Jersey, ed. 2, 1972).
27. Y. Y. Kagan and L. Knopoff, *J. Geophys. Res.* **86**, 2853 (1981).
28. Y. Ogata, *J. Phys. Earth* **31**, 115 (1983).
29. ———, *J. Am. Stat. Assoc.* **83**, 9 (1988).
30. The empirical (isotropic) spatial distribution of strong aftershocks in California was determined from the California data. The median distance between $M \geq 5.0$ aftershocks and their mainshock epicenter is 5 km. The 80 percentile distance is 9 km.

31. We thank M. V. Matthews for providing technical assistance throughout the study, B. Ellsworth and Y. Ogata for helpful discussions and suggestions, and R. D. Brown, for initially stimulating our interest in this problem.

20 September 1988; accepted 23 December 1988

---

# Time and Spatial Dependence of the Concentration of Less Than $10^5$ Microelectrode-Generated Molecules

STUART LICHT, VINCE CAMMARATA, MARK S. WRIGHTON*

**The time and spatial dependence of the concentration of as few as 40,000 electrogenerated, redox-active molecules has been determined. The distance between generator and detector microelectrodes in an array used in the study could be varied from 0.8 to 28 micrometers. Measurements of a sufficiently small ensemble of molecules allowed the experimental results to be compared with a quantitative simulation of the random movement of each member of the ensemble. The transit time of an electrogenerated species from the generator to a collector microelectrode was measured as a function of viscosity, diffusivity, and distance.**

MICROELECTROCHEMICAL DEVICES can be used in the study of catalysis, energy conversion, sensors, displays, and molecule-based electronics (*1–4*). In 1984 Kittlesen and Wrighton introduced the microfabrication of arrays of closely spaced, individually addressable micrometer-dimensioned electrodes (*5*) and their subsequent modification to fabricate molecule-based transistors, diodes, and sensors (*6*). In biological systems in which electrochemical stimulation or monitoring is useful, such as in the release of drugs and neurotransmitters (*7*), the use of microelectrodes may prove useful for creating and monitoring chemical signals. Another goal of such research is to reduce the size of the ensemble of electrogenerated species so that discrete electrochemical events can be measured.

We have used an array of closely spaced (~1 μm), individually addressable microelectrodes ($<10^{-7}$ cm$^2$ in area) to monitor the time and spatial dependence of $<10^5$ electrogenerated species. We have directly measured the dynamics associated with diffusing species on a sufficiently small scale (<30 μm) and of sufficiently few species ($<10^5$) that the measurements can be compared with a quantitative simulation of the random movement of each species. Studies of the dynamics of electrogenerated species in the solid state and other media not accessible by traditional electrochemical methods, such as rotating ring-disk electrodes, should now be possible (*8*).

Electrochemical methods have been used to monitor the diffusion of electrogenerated species. The concentration profile within the diffusion layer near a macroelectrode can be mapped to within ~5 μm with a movable light source (*9*) or a movable microelectrode (*10*). Microelectrodes have been used to monitor the time of flight of a pulse of $10^{-6}$ C through a variety of thin films overcoating the microelectrodes (*11*). Our smaller microelectrodes allow these diffusion studies to be extended to a qualitatively smaller amount of electrogenerated material.

Recently, Bard *et al.* demonstrated that in steady-state experiments a large fraction of redox-active material generated at one microelectrode can be detected or "collected" at nearby microelectrodes (*12*). We show here that the transit time for movement of the electrogenerated species from generator to collector is a measure of the diffusion characteristics of the electrogenerated solution species. A redox-active species is generated at one electrode, diffuses, and is collected at a second electrode (Scheme 1). Procedures used in the microfabrication and pretreatment of the gold microelectrode arrays are similar to those described in (*13, 14*).

The experimental in situ spatial and tem-

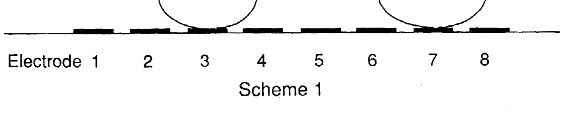

Scheme 1

**Scheme 1.** Representation of generation-collection experiments at a microelectrode array where "generation" can be effected at any one of the microelectrodes and "collection" can be done at any other microelectrode. The potential at electrode 3 is pulsed to "generate" an ensemble of reduced species. The potential at electrode 7 is fixed to "collect" a fraction of the reduced species by oxidation.

---

Department of Chemistry, Massachusetts Institute of Technology, Cambridge, MA 02139.

*To whom correspondence should be addressed.

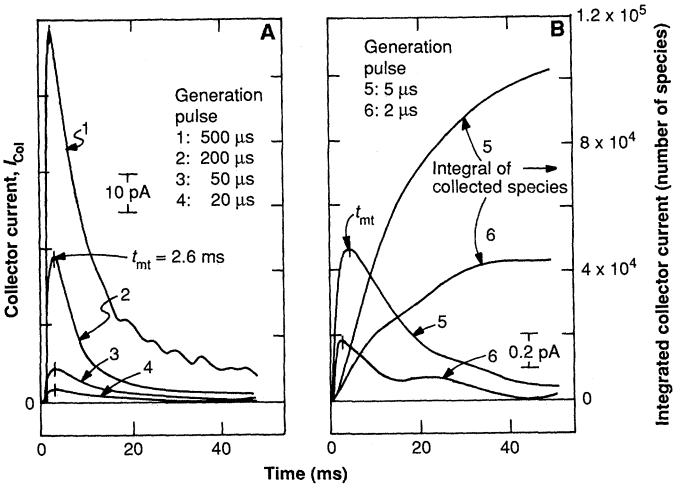

**Fig. 1.** (**A**) Plot of $I_{Col}$ versus time for electrogenerated $Ru(NH_3)_6^{2+}$ from pulses of $4 \times 10^{-12}$ to $1.6 \times 10^{-14}$ C at a generator microelectrode 1.3 µm wide by 6 µm long. $I_{Col}$ corresponds to oxidation at a parallel collector microelectrode (of the same size as the generator) separated by a gap of 0.8 µm. The collector electrode was maintained at 0.0 V versus the standard calomel electrode (SCE). Experiments were conducted in 10 m*M* $Ru(NH_3)_6Cl_3$ in 0.1*M* aqueous KCl. The generator electrode was pulsed from 0.0 to −0.4 V versus SCE, for durations varying from 2 to 500 µs, which resulted in a 8-nA cathodic current pulse at the generator. (**B**) Time dependence of the integrated collector current and $I_{Col}$ versus time for the 2- and 5-µs generation pulses. Current spikes caused by capacitive coupling from the pulsed generator electrode are omitted for clarity.

poral distribution of electrogenerated redox-active species is illustrated with measurements of the generation (Eq. 1) and collection (Eq. 2) of $Ru(NH_3)_6^{2+}$:

$$Ru(NH_3)_6^{3+} \xrightarrow{+e^-} Ru(NH_3)_6^{2+} \qquad (1)$$

$$Ru(NH_3)_6^{2+} \xrightarrow{-e^-} Ru(NH_3)_6^{3+} \qquad (2)$$

The microelectrode array is immersed in an electrolyte solution containing $Ru(NH_3)_6^{3+}$ as the only active species. Initially, microelectrodes termed "generator" and "collector" are maintained at $E_{ox}$, a potential positive of $E^{\circ\prime}$ [$Ru(NH_3)_6^{3+/2+}$]. The generator is then pulsed to a reducing potential, $E_{red}$, which creates $Ru(NH_3)_6^{2+}$ in a process that is monitored by a cathodic current $I_{Gen}$. Of the generated $Ru(NH_3)_6^{2+}$, 71% escapes from the generator in a pulse from $E_{ox}$ to $E_{red}$ and back to $E_{ox}$ (*8*). As the $Ru(NH_3)_6^{2+}$ diffuses away from the generator, the time variation of the current at the collector, $I_{Col}$, signals the arrival, collection, and regeneration of $Ru(NH_3)_6^{3+}$. Alternatively, movement of $Ru(NH_3)_6^{3+}$ may be studied through the application of an oxidizing potential in an electrolyte that initially contains only $Ru(NH_3)_6^{2+}$. Our results demonstrate that $I_{Col}$ is proportional to the concentration of the relevant redox species, so that the time dependence of $I_{Col}$ at a given collector yields time-dependent concentration data for the electrogenerated species. Independent measures of $I_{Col}$ versus time at different collectors allow mapping of the spatial dependence of the concentration at a given time.

Typical measurements of $I_{Col}$ versus time are presented in Fig. 1 for $Ru(NH_3)_6^{2+}$ generated with square-wave pulses and collected at two microelectrodes separated by 0.8 µm. The collection efficiency $\Phi_{ss}$, which is the ratio of collected species to generated species (*12*), is ~0.40 (independent of generation pulse time) from the integrated $I_{Col}$. The time dependence of the collection of as little as $7 \times 10^{-20}$ mol, or 40,000 $Ru(NH_3)_6^{2+}$ ions, is shown. The relevant dynamic parameter is the transit time, $t_{mt}$, which is taken to be the time at which one observes the maximum value of $I_{Col}$. We can routinely measure $I_{Col}$ as low as $10^{-13}$ A to a time resolution of 1 ms, which gives an integrated resolution of $10^{-16}$ C ($10^{-21}$ mol, or less than 1000 ions). By taking $t = 0$ to be the midpoint of the generation pulse, we find that $t_{mt}$ is 2.6 ± 0.3 ms (range from sets of 10 independent trials) for the 0.8-µm gap between generator and collector electrodes and is independent of the generator pulse time. We used typical generator pulse times that were less than one-third of the expected value of $t_{mt}$ to reduce complications from "feedback" (*12*).

Data in Fig. 1 illustrate the concept of pulsed generation-collection experiments, but complications in relating $t_{mt}$ to the diffusivity occur in that the width of the generator microelectrode (1.3 µm) is greater than the gap (0.8 µm) separating it from the collector. We related $t_{mt}$ to diffusivity by measuring $t_{mt}$ for transit across an array of seven collector microelectrodes (Fig. 2). Each one of the eight microelectrodes is 2.7 µm wide, and they are separated from each other by 1.4 µm. We adjusted the distance *d*, the separation from the center of the generator to the nearest edge of the activated collector, by collecting at one of the seven collector electrodes. For the $Ru(NH_3)_6^{3+/2+}$ experiments, the plot of $t_{mt}$ versus $d^2$ was essentially linear, as expected for diffusion. For a diffusional process, $t_{mt}$ should be proportional to $1/D$, where *D* is the diffusion coefficient. By varying the sucrose content of the aqueous $Ru(NH_3)_6^{3+/2+}$ solution, we varied *D* in a systematic fashion (*15*). Results of measurements of $t_{mt}$ for several sucrose solutions (Fig. 2) show that $t_{mt} \propto 1/D$. An absolute value of *D* for $Ru(NH_3)_6^{2+}$ in 0.1*M* $NaClO_4$ was determined from limiting currents at a 25-µm microdisk electrode. Thus the $Ru(NH_3)_6^{3+/2+}$ experiments are consistent with Eq. 3:

$$t_{mt} = 0.22\, d^2/D \qquad (3)$$

The constant of proportionality for an array of parallel "band" microelectrodes is 0.22 ± 0.02. Thus, for this geometry, $t_{mt}$ can be used with Eq. 3 to determine *D*. The concentration of the diffusing species need not be accurately known with this method.

Cytochrome c illustrates how our technique can be used to measure *D*. This molecule has been characterized by the spreading of the sedimentation boundary of an ultracentrifuged sample (*16*), cyclic voltammetry (*17*), and rotating disk voltammetry (*18*). Although the generally accepted value of *D* for cytochrome c is $1.1 \times 10^{-6}$ cm²/s, values from various modified electrode methods span the range from $1.8 \times 10^{-7}$ to $11 \times 10^{-7}$ cm²/s (*17–20*). Our technique is a direct measurement and should be independent of the electrode material used. Our $t_{mt}$ values for ferrocytochrome c yielded $D = 1.1 \times 10^{-6}$ cm²/s, consistent with the accepted values obtained with rotating disk

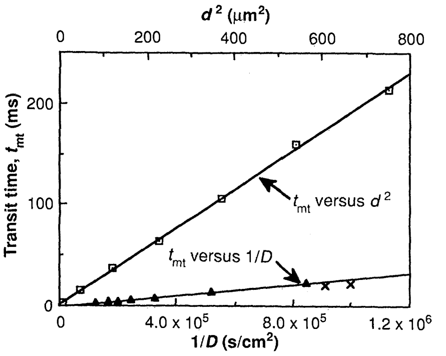

**Fig. 2.** Plots of $t_{mt}$ versus $d^2$ (upper scale, ☐) and $t_{mt}$ versus 1/*D* (lower scale, ▲) for $Ru(NH_3)_6^{2+}$ generated at 20°C in 2.5 m*M* $Ru(NH_3)_6^{3+}$, 0.1*M* $NaClO_4$, *p*H 6.5, buffer by a generation sequence from 0.0 to −0.4 V and back to 0.0 V versus SCE. The collector microelectrode was held at 0.0 V versus SCE. We achieved variation in *d* by using collector electrodes situated at different distances from the generator (Scheme 1), in an array of eight, parallel microelectrodes 70 µm long by 2.7 µm wide separated from each other by 1.4 µm. We achieved a variation in *d* from $7.8 \times 10^{-6}$ to $1.26 \times 10^{-7}$ cm²/s by adding sucrose (*15*); $t_{mt}$ versus 1/*D* was measured for adjacent microelectrodes as generator and collector. Data for ferri- and ferrocytochrome c (×) at 24°C in 0.1*M* $NaClO_4$, *p*H 6.5, with 1,2-*bis*(4-pyridyl)ethylene (*19*) are included in the plot of $t_{mt}$ versus 1/*D*.

voltammetry (*18*) and chronoabsorptometry (*20*) (Fig. 2). We also found $D = 1.0 \times 10^{-6}$ cm$^2$/s for ferricytochrome c. Because the relative errors in our measurements are sufficiently small, we conclude that there is an experimentally significant difference for $D$ between the reduced and the oxidized forms of cytochrome c.

We were interested in quantitatively simulating generation-collection experiments in order to better understand the concentration evolution with time. However, in the analysis of mass transport to and from small electrodes, discontinuities occur at the microelectrode edges where the diffusion-limited flux for a reversible system is infinite (*21*). Thus, we chose to describe the diffusion numerically with the simpler Einstein-Smoluchowski random walk rather than analytically with Fick's laws. A two-dimensional digital simulation (in the plane normal to the array) was used. Simulated concentration profiles of the generated species are shown in Fig. 3 for a generation-collection experiment similar to that summarized by data in Fig. 2. The simulation accurately describes the variation in $\Phi_{ss}$ values upon changes in (i) collector symmetry, (ii) collector width, (iii) distance from the generator electrode, and (iv) diffusion coefficient. Subsequent to a generation pulse, the peak of $I_{Col}$ (the maximum collection rate) occurs at a time $t_{mt}$ according to Eq. 4 for band microelectrodes:

$$t_{mt}\ (\text{simulation}) = (0.20)d^2/D \qquad (4)$$

The simulation size, $10^4$ random particles, closely approximates the actual number of species generated in our experiments. The simulation accurately predicts our experimental determination of the $D$ and $d$ dependence of $t_{mt}$ (Eq. 3) (*14*).

Our studies demonstrate an experimental and theoretical methodology suitable for investigating the diffusion of redox-active molecules in solution. If the interelectrode separation is reduced to <0.1 μm by shadow deposition techniques (*22*), the values of $t_{mt}$ should decrease by a factor of ~100, whereas the peak value of $I_{Col}$ should increase by the same factor for a given number of generated species. In principle, our measurements of ~40,000 species (Fig. 1B) could be extended to as few as several hundred. Smaller interelectrode spacings would also allow more convenient measure of $D$ for situations where $D$ is small, as in solid-state electrolytes (*23*). Because $D$ and solution viscosity are related according to Eq. 5 (*24*), measurements of $t_{mt}$ allow determination of viscosity, $\eta$,

$$D = z_i e_0 / 6 \pi k T r \eta \qquad (5)$$

where $z_i$ is the charge on the ion, $e_0$ is the fundamental unit of charge, $k$ is Boltzmann's constant, $T$ is temperature, and $r$ is the Stokes radius of the ion. Such arrays may be useful in probing local versus global viscosity (*25*). For polymers, solid electrolytes, and gels, our techniques should provide useful information on the diffusivity and local environments of redox-active materials for which hydrodynamic techniques (*8*) may not be suitable.

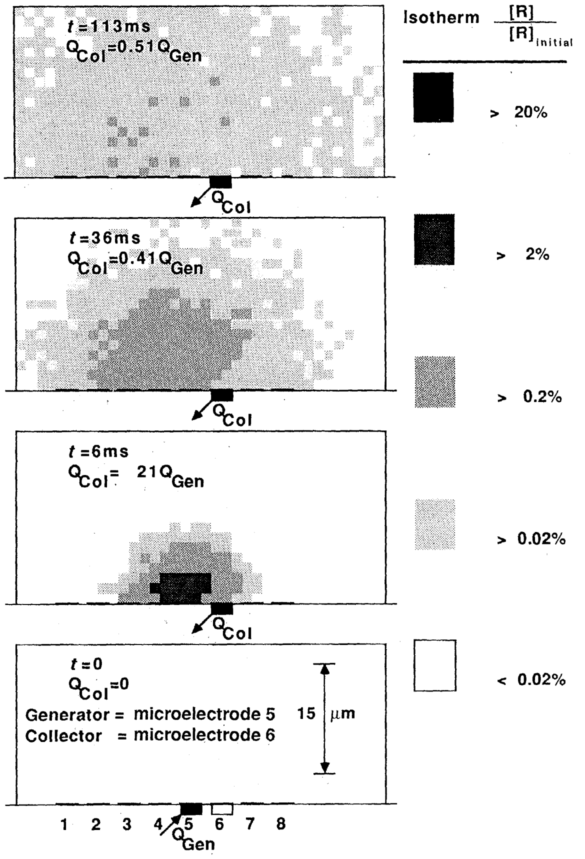

**Fig. 3.** A two-dimensional random walk simulation of ion movement and collection efficiencies in generator-collector microelectrode experiments where the geometry is as in Fig. 2. A cross-sectional plane perpendicular to the length of the eight parallel microelectrodes is depicted in which a pulse of 10,000 diffusing species, $Q_{Gen}$, is introduced at the indicated generator site. The concentration profile of the 10,000 species is shown at $t$ = 0, 6, 36, and 113 ms after initiation of a random walk by each species. $R/R_{initial}$ is a measure of the concentration profile. Only the central 20% of the numerically modeled active grid area is indicated. The species can make discrete random movements among sites on a grid. We chose $D$ to be $7.8 \times 10^{-6}$ cm$^2$/s to simulate diffusion of $Ru(NH_3)_6^{2+}$ in $H_2O$. Each species moves randomly along the grid an incremental distance $\Delta X$ or $\Delta Y$ of 1.37 μm during each iterative time cycle, $\Delta t$, where $\Delta t$ is the average time needed for a given species to move a distance $\Delta X$; $\Delta t = (\Delta X)^2/4D$ (*24*). Diffusing species that arrived at the collector site were counted as $Q_{Col}$ and removed from solution to indicate electron injection into the collector. The collection flux (equivalent to the normalized $I_{Col}$ in our experiments) versus time and the total (integrated) collection flux can be computed. The computed collection efficiencies, $\Phi_{ss}$, 0.21, 0.41, and 0.51 at 6, 36, and 113 ms, respectively, are in good accord with experiment. The simulations of $I_{Col}$ versus time give $t_{mt}$ values ~10% less than experiment.

## REFERENCES AND NOTES

1. M. S. Wrighton, *Science* **231**, 32 (1986).
2. C. E. D. Chidsey and R. W. Murray, *ibid.*, p. 25.
3. L. R. Faulkner, *Chem. Eng. News* **62** (no. 9), 28 (1984).
4. R. M. Wightman, *Science* **240**, 415 (1988); *Anal. Chem.* **53**, 1125A (1981).
5. G. Kittlesen and M. S. Wrighton, *J. Am. Chem. Soc.* **106**, 5375 (1984).
6. S. Chao and M. S. Wrighton, *ibid.* **109**, 2197 (1987).
7. A. N. K. Lau *et al.*, *ibid.* **105**, 5278 (1983); B. Zinger and L. L. Miller, *ibid.* **106**, 6861 (1984).
8. A. J. Bard and L. R. Faulkner, *Electrochemical Methods* (Wiley, New York, 1980); S. Bruckenstein and B. J. Feldman, *J. Electroanal. Chem.* **9**, 395 (1965).
9. P. Rossi, C. W. McCurdy, R. L. McCreery, *J. Am. Chem. Soc.* **103**, 2524 (1981); C.-C. Jan and R. L. McCreery, *Anal. Chem.* **58**, 2771 (1986).
10. R. C. Engstrom, M. Weber, D. J. Wunder, R. Burgess, S. Winquist, *Anal. Chem.* **58**, 844 (1986); R. C. Engstrom, T. Meaney, R. Tople, R. M. Wightman, *ibid.* **59**, 2005 (1987).
11. B. J. Feldman, S. W. Feldberg, R. Murray, *J. Phys. Chem.* **91**, 6558 (1987).
12. A. J. Bard *et al.*, *Anal. Chem.* **58**, 2321 (1986).
13. M. S. Wrighton *et al.*, in *Chemically Modified Surfaces in Science and Industry*, D. E. Leyden and W. T. Collins, Eds. (Gordon and Breach, New York, 1988), p. 337.
14. S. Licht *et al.*, unpublished results.
15. X. Zhang *et al.*, *J. Am. Chem. Soc.* **109**, 1916 (1987).
16. A. Ehrenberg, *Acta Chem. Scand.* **11**, 1257 (1957).
17. I. Taniguchi *et al.*, *J. Chem. Soc. Chem. Commun.* **1982**, 1032 (1982).
18. W. J. Albery, M. J. Eddowes, H. A. O. Hill, A. R. Hillmary, *J. Am. Chem. Soc.* **103**, 3904 (1981).
19. M. J. Eddowes and H. A. O. Hill, *ibid.* **101**, 4461 (1979); I. Taniguchi, M. Iseki, K. Toyosawa, H. Yamaguchi, K. Yasukouchi, *J. Electroanal. Chem.* **164**, 385 (1984); M. A. Harmer and H. A. O. Hill, *ibid.* **170**, 1369 (1984).
20. E. F. Bowden *et al.*, *J. Am. Chem. Soc.* **104**, 7641 (1982).
21. S. Pons and M. Fleishman, *Anal. Chem.* **59**, 1391A (1987).
22. E. T. T. Jones, O. M. Chyan, M. S. Wrighton, *J. Am. Chem. Soc.* **109**, 5526 (1987).
23. V. Cammarata *et al.*, unpublished results.
24. A. Einstein, *Investigations on the Theory of the Brownian Movement* (Methuen, London, 1926).
25. K. L. Yam, D. K. Anderson, R. E. Buxbaum, *Science* **241**, 330 (1988); A. F. Olea and J. K. Thomas, *J. Am. Chem. Soc.* **110**, 4494 (1988).
26. Supported in part by the Office of Naval Research, the Defense Advanced Research Projects Agency, and Lockheed Missiles and Space Company.

7 October 1988; accepted 27 December 1988